Supplement of Geosci. Model Dev., 18, 8627–8649, 2025
https://doi.org/10.5194/gmd-18-8627-2025-supplement

Geoscientific Model Development
Open Access

Supplement of

The Speciated isoprene emission model with the MEGAN algorithm for China (SieMAC)

Shengjun Xi et al.

Correspondence to: Yuhang Wang (yuhang.wang@eas.gatech.edu)

Supplement

Tables

Table S1. The standard emission rates of isoprene (ER) and specific leaf area (SLA) for species used in this study. Emission Factor (EF) is: $EF = ER/SLA$.

Species	ER (μg C g^{-1} h^{-1})	SLA (cm^2 g^{-1})	EF (μg C m^{-2} h^{-1})
	Broadleaf	***Evergreen***	***Trees***
Acacia confusa	0.8[1]	100[2]	80
Albizia chinensis	0.1[3][4]	100[2]	10
Areca catechu	70[5]	100[2]	7000
Bambusa	32.3[3][6]	277[7]	1166.1
Bombax ceiba	0.1[1]	211.6[8]	4.7
Castanea seguinii	0[9]	/	0
Castanopsis	1.4[10]	51.6[7][11]	271.3
Cercis chinensis	7.2[10]	100[2]	720
Choerospondias axillaris	0.1[1]	205[12]	4.9
Chukrasia tabularis	0.1[1]	100[2]	10
Cinnamomum camphora	0.2[3][6]	100[2]	20
Cocos nucifera	63.1[13]	100[2]	6310
Cryptocarya chinensis	95.9[1]	100[2]	9590
Cyclobalanopsis	278.9[3]	100[2]	27890
Dendrocalamus	70[1]	100[2]	7000
Dipterocarpus	0.1[1]	100[2]	10
Dysoxylum	0.1[1]	100[2]	10
Elaeocarpus decipiens	11.9[14]	100[2]	1190
Eucalyptus	60[15]	100[2]	6000
Fargesia	4.3[10]	100[2]	430
Ficus benjamina	9.4[3]	120.1[8]	782.7
Ficus microcarpa	1.4[1]	120.1[8]	116.6
Ficus (other)	70[1]	120.1[8]	5828.5

Garcinia paucinervis	0.1[1]	100[2]	10
Hevea brasiliensis	2.6[3]	100[2]	260
Indocalamus tessellatus	4.3[10]	100[2]	430
Lithocarpus	1.5[16]	97[12]	154.6
Madhuca pasquieri	69.5[17]	100[2]	6950
Michelia figo	0.1[3]	100[2]	10
Neosinocalamus affinis	35.2[18]	48.3[19]	7287.8
Phellodendron amurens	0.1[1]	100[2]	10
Phyllostachys edulis	102.2[10][20]	250[7]	4088
Phyllostachys (other)	70[1][15][21]	250[7]	2800
Pleioblastus amarus	75.8[10]	179.2[22]	4229.9
Podocarpus imbricatus	0[1]	/	0
Pometia pinnata	2.5[3]	100[2]	250
Pseudosasa	32.3[3]	100[2]	3230
Qiongzhuea tumidinoda	32.3[3]	100[2]	3230
Schima argentea	0.1[1]	112[7]	8.9
Schima wallichii	0[1]	/	0
Sterculia lanceolata	0.1[1]	100[2]	10
Terminalia	0[3]	/	0
Yushania	32.3[3]	20[19]	16150
Others	1.5[16]	100[2]	150
	Broadleaf	***Deciduous***	***Trees***
Acer pictum subsp. mono	0[1]	/	0
Acer (other)	0.1[1]	230.7[23]	4.3
Alnus nepalensis	0.1[1]	100[2]	10
Amygdalus persica	10.6[24]	100[2]	1060
Armeniaca	7.0[24]	100[2]	700
Betula ermanii	0[1]	/	0
Betula platyphylla	0.1[1]	198[25]	5.1
Betula luminifera	0.1[1]	145.4[7]	6.9

Betula utilis	0.1[1]	217.1[23]	4.6
Betula (other)	0.1[1][13]	113[9]	8.8
Dalbergia hupeana	30.1[10]	100[2]	3010
Diospyros kaki	0.2[24]	100[2]	20
Fagus	0.1[15]	83[12]	12
Fraxinus	0.1[1]	95.7[26]	10.4
Ginkgo biloba	0[3][6]	/	0
Juglans mandshurica	0[1]	/	0
Juglans regia	3.1[24]	100[2]	310
Liquidambar formosana	65.5[10]	162[12]	4043.2
Malus sieversii	0.9[3][6]	152[9]	59.2
Morus alba	0.1[1]	100[2]	10
Phellodendron	0.1[1]	100[2]	10
Populus simonii	191.1[27]	100[2]	19110
Populus suaveolens	40[1] [28]	100[2]	4000
Populus (other)	105.8[6]	158.6[7][29]	6671
Pyrus	0.3[24]	100[2]	30
Quercus liaotungensis	98.9[1]	100[2]	9890
Quercus aliena	65.5[9]	106.9[9]	6127.2
Quercus dentata	32.1[9]	106.9[9]	3002.8
Quercus variabilis	65.5[9][29]	99.2[29]	6602.8
Quercus glandulifera	196[10]	159[7]	12327
Quercus (other)	70[1][15]	100[2]	7000
Robinia	49.8[29]	100[2]	4980
Salix	70.2[3]	150.6[29]	4661.4
Sassafras tzum	0.1[28]	100[2]	10
Tilia	0.1[1]	64.2[26]	15.6
Ulmus	0.3[3][6]	142.7[29]	21
Others	1.5[16]	100[2]	150
	Needleleaf	***Evergreen***	***Trees***

Abies	0.1[1]	28.3[7]	35.3
Casuarina equisetifolia	2.9[3]	150[2]	193.3
Cryptomeria fortunei	0.6[3]	150[2]	40
Cunninghamia lanceolata	0.1[15]	61[7]	16.4
Cupressus funebris	0.1[3]	150[2]	6.7
Juniperus	0.1[1]	150[2]	6.7
Keteleeria fortunei	0.1[28]	150[2]	6.7
Picea jezoensis Carr. var. microsperma	7.2[1]	14[7]	5142.9
Picea (other)	8[6][12]	14[6]	5714.3
Pinus armandii	0[1][13]	/	0
Pinus bungeana	0[6]	/	0
Pinus koraiensis	0[3]	/	0
Pinus massoniana	0.7[3][7]	51.5[7]	135.9
Pinus pumila	0.1[1]	64.1[7]	15.6
Pinus yunnanensis	0[1][13]	/	0
Pinus (other)	0.4[3][6]	64.1[7][29]	62.4
Platycladus orientalis	0[1]	/	0
Sabina przewalskii	0.1[3]	34.7[30]	28.8
Tsuga	0.1[15]	75[31]	13.3
Others	1.5[16]	150[2]	100
	Needleleaf	***Deciduous***	***Trees***
Larix gmelinii	0[3]	/	0
Larix olgensis	0[1]	/	0
Larix principis-rupprechtii	7.4[1]	113[7]	654.9
Larix (other)	0.1[1]	113[7]	8.8
Metasequoia glyptostroboides	0[32]	/	0
Taxodium distichum	0.5[1]	150[2]	33.3
Others	1.5[16]	150[2]	100
		Shrubs	

Acacia farnesiana	0.1[1][4]	112.4[9]	8.9
Alchornea trewioides	0.1[1]	131[33]	7.6
Amygdalus mongolica	10.6[24]	112.4[9]	943.1
Armeniaca sibirica	7[24]	70[9]	1000
Baeckea frutescens	10[34]	112.4[9]	889.7
Bauhinia championii	70[1]	90[35]	7777.8
Bauhinia faberi	70[1]	112.4[9]	6227.8
Berberis	14[1]	112.4[9]	1245.6
Caragana	0.1[1]	10.9[36]	91.7
Castanea	0[9]	/	0
Cipadessa cinerascens	0.1[1]	112.4[9]	8.9
Corylus heterophylla	0.1[1]	112.4[9]	8.9
Cotinus coggygria Scop.	0.1[1]	122.3[37]	8.2
Croton argyratus	0.1[1]	112.4[9]	8.9
Desmos chinensis	0[5]	/	0
Dracaena cambodiana	0.1[1]	318[38]	3.1
Elaeagnus pungens	1.5[16]	152[39]	98.7
Gleditsia microphylla	0.3[40]	112.4[9]	26.7
Hippophae rhamnoides	1.5[16]	43.9[41]	341.7
Juniperus squamata	0.1[1]	112.4[9]	8.9
Lespedeza	35.6[10]	255.4[42]	1393.9
Liquidambar formosana	65.5[10]	162[12]	4043.2
Litsea populifolia	0.1[1]	180[43]	5.6
Loropetalum chinense	1.5[16]	117[12]	128.2
Macaranga denticulata	0.1[1]	112.4[9]	8.9
Mallotus barbatus	0.1[1]	112.4[9]	8.9
Malus baccata	1.5[16]	65.8[9]	228
Ostryopsis davidiana	1.5[16]	117[42]	128.2
Phyllanthus	0.1[1]	112.4[9]	8.9
Pinus yunnanensis var. pygmaea	0[13]	/	0

Potentilla	1.5[16]	50[44]	300
Psidium guajava	1.5[16]	67.3[31]	222.9
Quercus fabri	40[28]	232[12]	1724.1
Quercus glandulifera	196[10]	159[7]	12327
Quercus (other)	40[28]	112.4[9]	3558.7
Rhododendron przewalskii	0.1[1]	80[35]	12.5
Rhododendron simsii	0.1[1]	112.4[9]	8.9
Rhododendron (other)	0.1[1]	42.5[45]	23.5
Rhus chinensis	0.2[1][13]	180[46]	11.1
Rosa	0.1[1]	84.8[41]	11.8
Sabina	0.1[3]	34.7[30]	28.8
Salix	70.2[3]	150.6[2]	4661.4
Sibiraea angustata	1.5[16]	141.9[47]	105.7
Sophora moorcroftiana	1.5[16]	41.8[41]	358.9
Spiraea	0.1[1]	145.8[42]	6.9
Syringa	0.2[6]	173.5[8]	11.5
Tamarix	1.5[16]	22.5[48]	666.7
Vitex negundo	1.5[16]	170[35]	88.2
Others	1.5[16]	112.4[9]	133.5

Table S2. The monthly averaged PFT-ecoregion dependent base LAIs for eight ecoregions in Fig. S2. These base LAI values are used to derive PFT LAIs at each grid cell.

Ecoregion	PFT	May	Jun	Jul	Aug	Sept
Boreal conifer forest	*Broadleaf evergreen tree*	/[a]	/	/	/	/
	Broadleaf deciduous tree	2.2	5	5	5	2.6
	Needleleaf evergreen tree	2.9	5	5	5	3.0
	Needleleaf deciduous tree	2.7	5	5	5	2.3
	Shrub	1.0	2.6	3.2	2.3	1.0

	Crop	0.7	2.7	4	4	1.3
	Grass	1.0	4	4	4	1.8
Temperate mixed forest	*Broadleaf evergreen tree*	/	/	/	/	/
	Broadleaf deciduous tree	2.4	5	5	5	5
	Needleleaf evergreen tree	2.8	5	5	5	4.1
	Needleleaf deciduous tree	2.4	5	5	5	2.6
	Shrub	2.1	4	4	4	2.5
	Crop	0.5	1.4	4	4	2.1
	Grass	0.9	2.0	3.6	3.8	2.0
Temperate deciduous forest	*Broadleaf evergreen tree*	2.6	3.2	4.8	7	6.3
	Broadleaf deciduous tree	5	5	5	5	5
	Needleleaf evergreen tree	4.3	5	5	5	5
	Needleleaf deciduous tree	3.5	5	5	5	4.7
	Shrub	4	4	4	4	4
	Crop	1.4	2.0	3.1	4	2.0
	Grass	1.5	3.1	4	4	2.6
Subtropical evergreen forest	*Broadleaf evergreen tree*	7	7	7	7	7
	Broadleaf deciduous tree	5	5	5	5	5
	Needleleaf evergreen tree	5	5	5	5	5
	Needleleaf deciduous tree	5	5	5	5	5
	Shrub	2.0	3.0	3.3	4	3.2

	Crop	1.6	1.8	3.5	4	2.5
	Grass	1.3	2.2	3.1	3.3	2.4
Tropical monsoon forest	*Broadleaf evergreen tree*	7	7	7	7	7
	Broadleaf deciduous tree	5	5	5	5	5
	Needleleaf evergreen tree	3.4	5	5	5	5
	Needleleaf deciduous tree	/	/	/	/	/
	Shrub	4	4	4	4	4
	Crop	2.0	2.4	2.7	3.2	3.3
	Grass	1.5	2.2	2.1	3.0	2.4
Steppes	*Broadleaf evergreen tree*	/	/	/	/	/
	Broadleaf deciduous tree	2.0	5	5	5	2.9
	Needleleaf evergreen tree	2.3	4.7	5	5	3.1
	Needleleaf deciduous tree	2.0	5	5	5	2.1
	Shrub	0.8	1.1	1.8	1.4	0.8
	Crop	0.6	1.6	4	4	1.8
	Grass	0.6	1.4	2.4	2.4	1.3
Desert	*Broadleaf evergreen tree*	7	7	7	7	5.9
	Broadleaf deciduous tree	5	5	5	5	3.7
	Needleleaf evergreen tree	3.7	4.9	5	4.5	3.0
	Needleleaf deciduous tree	4.1	5	5	4.9	2.8
	Shrub	0.6	0.6	0.6	0.7	0.6

	Crop	1.0	2.1	3.5	3.0	1.6
	Grass	0.8	1.3	1.7	1.5	0.9
High-mountain vegetation	*Broadleaf evergreen tree*	3.2	7	5.6	7	6.7
	Broadleaf deciduous tree	2.7	5	5	5	5
	Needleleaf evergreen tree	2.4	4.9	4.0	5	4.3
	Needleleaf deciduous tree	1.3	2.5	5	5	2.0
	Shrub	0.4	0.5	0.6	0.6	0.5
	Crop	1.2	2.7	4	3.5	1.8
	Grass	0.6	1.4	2.0	2.4	1.3

[a]: The PFT is not present in the ecoregion.

Figures

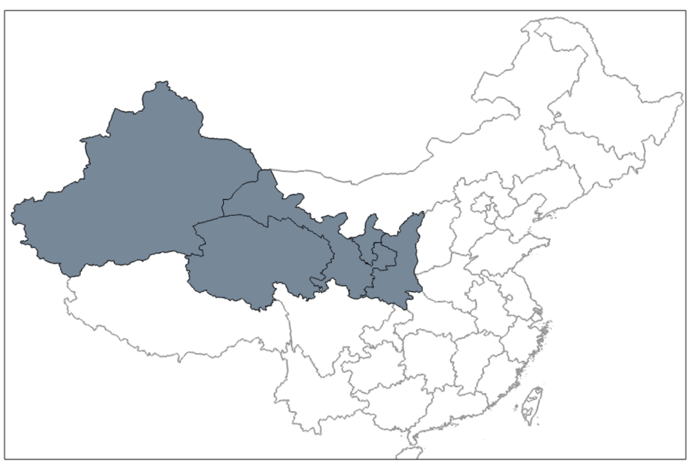

Figure S1. Region (shaded) in which the emission factor (EF) and temperature dependence were adjusted for grass. As discussed in Section 2.1 and 2.2.1.

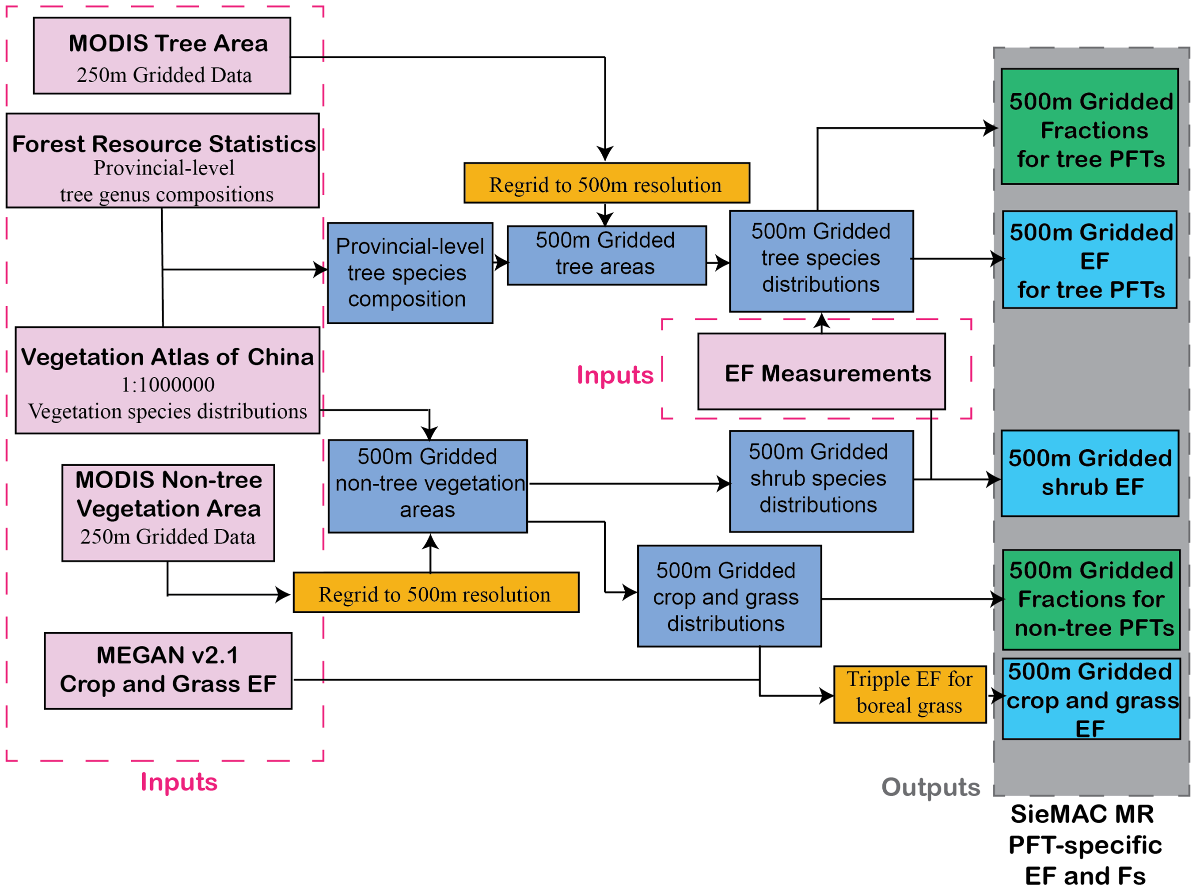

Figure S2. Data integration workflow for the MR approach, showing the integration of Forest Resource Statistics, Vegetation Atlas, and MODIS products.

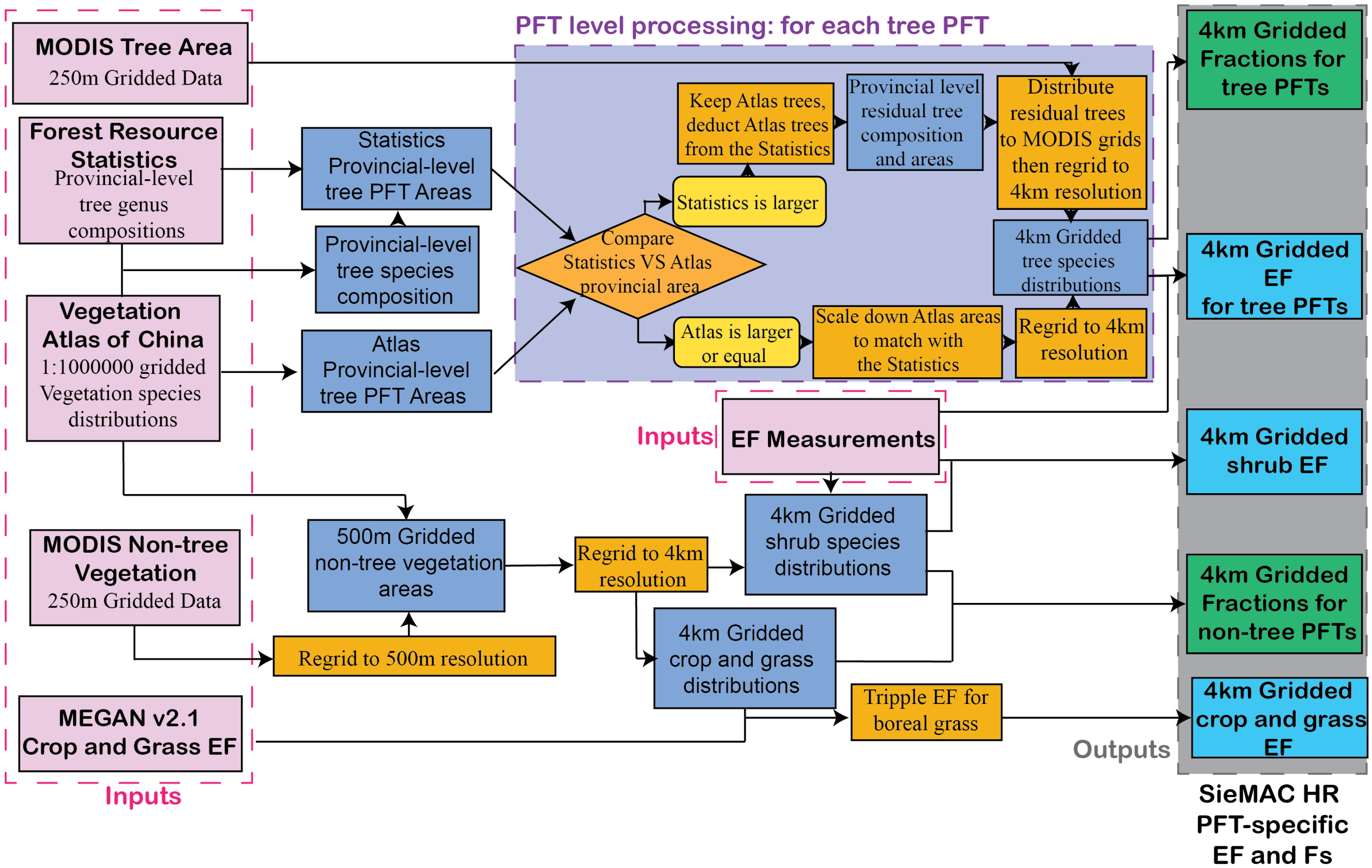

Figure S3. Data integration workflow for the HR approach, showing the MODIS-based methodology with simplified data requirements.

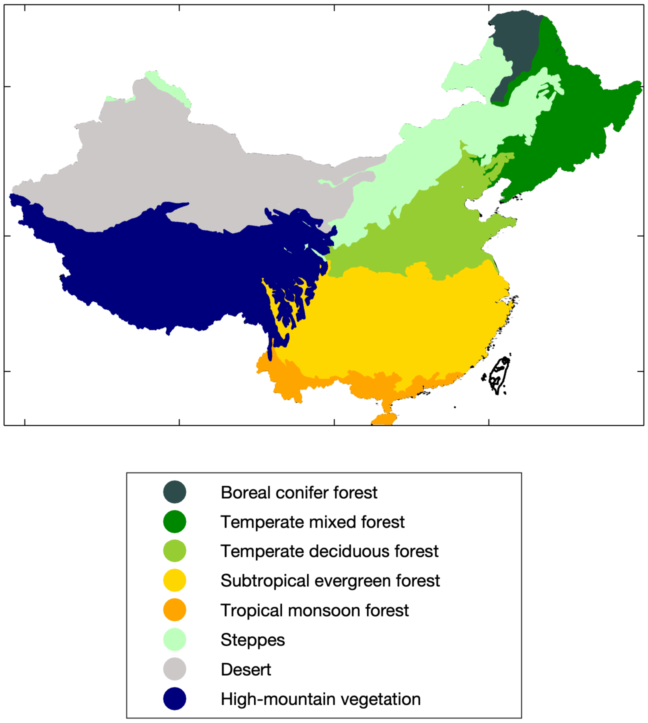

Figure S4. Ecoregion map used to assign region-specific PFT LAIs. Mainland China is divided into eight ecoregions: Boreal conifer forest, Temperate mixed forest, Temperate deciduous forest, Subtropical evergreen forest, Tropical monsoon forest, Steppes, Desert, High-mountain vegetation, following RodrÍguez and PÉrez (2013) and the Vegetation Atlas of China (Zhang, 2007).

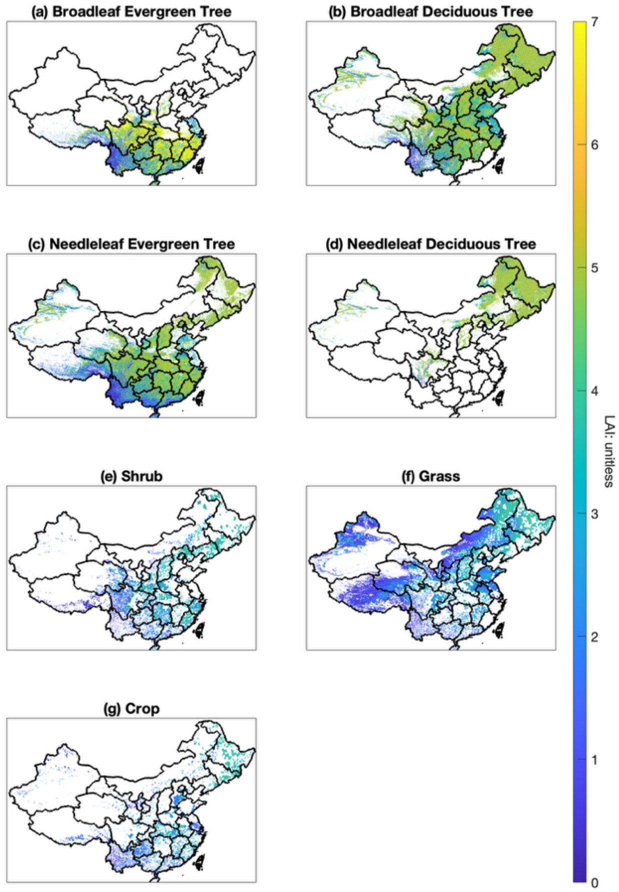

Figure S5. PFT-specific leaf area index (LAI) distributions of the MR approach for July 2013. This represents peak summer conditions when isoprene emissions are maximum.

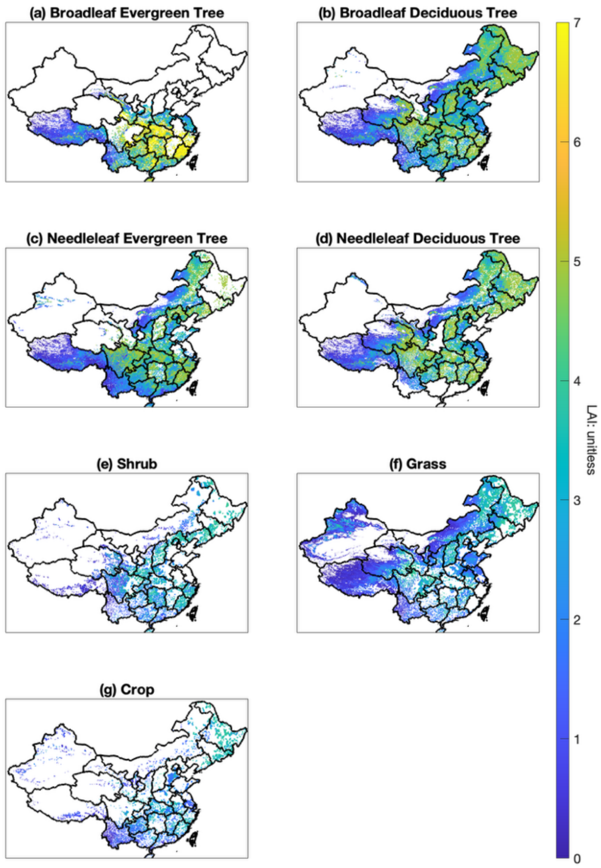

Figure S6. PFT-specific leaf area index (LAI) distributions of the HR approach for July 2013. This represents peak summer conditions when isoprene emissions are maximum.

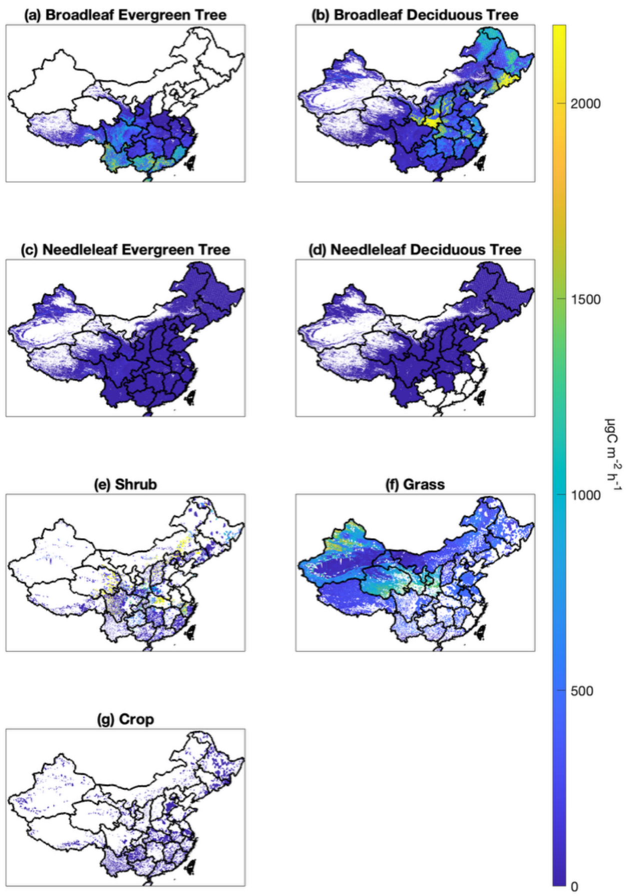

Figure S7. Combined emission factor and PFT fraction products (EF × fraction) for the MR approach. This represents the emission potential per unit area for each vegetation type.

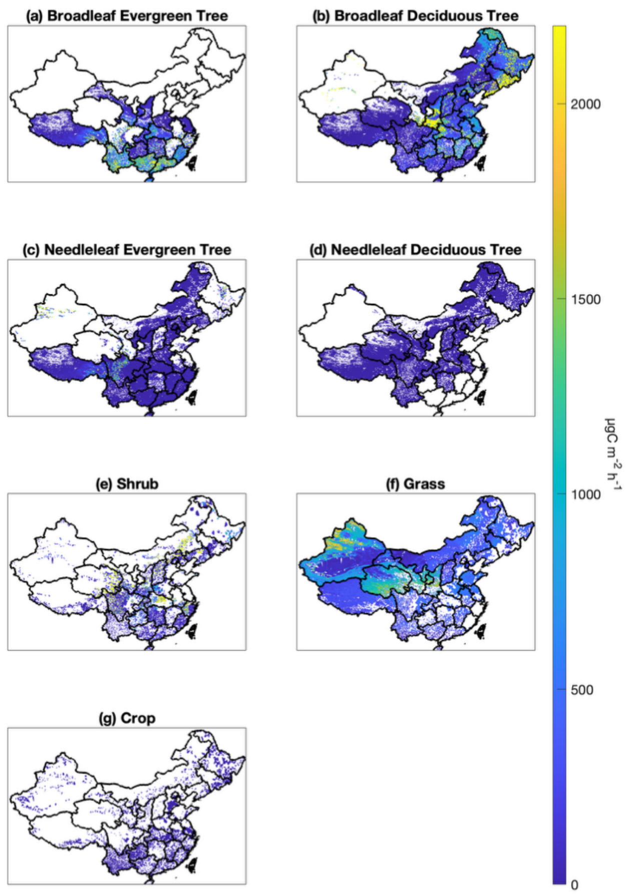

Figure S8. Combined emission factor and PFT fraction products (EF × fraction) for the HR approach. This represents the emission potential per unit area for each vegetation type.

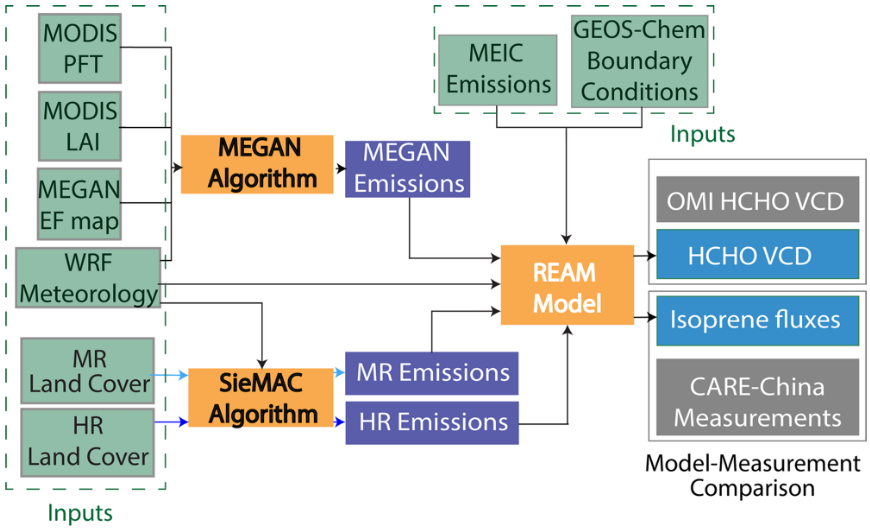

Figure S9. Schematic diagram of the REAM model setup showing the integration of SieMAC isoprene emissions and evaluation against observational datasets.

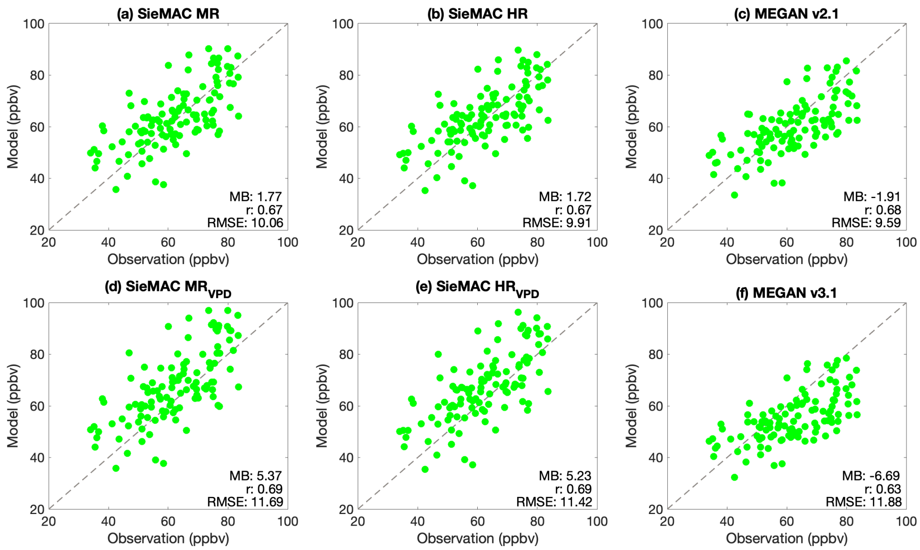

Figure S10. Evaluation of the REAM simulations for surface Ozone (O_3) during summer 2013. Scatterplots compare modeled site mean maximum daily 8-h average ozone (MDA8) with observations from the China National Environmental Monitoring Centre (CNEMC) network for six emission configurations: (a) SieMAC MR, (b) SieMAC HR, (c) MEGAN v2.1, (d) SieMAC MR$_{VPD}$, (e) SieMAC HR$_{VPD}$, and (f) MEGAN v3.1. Each point represents one monitoring site; the dashed line marks the 1:1 relation. Panel annotations list the mean bias (MB), root-mean-square error (RMSE), and Pearson correlation coefficient (r) for each configuration.

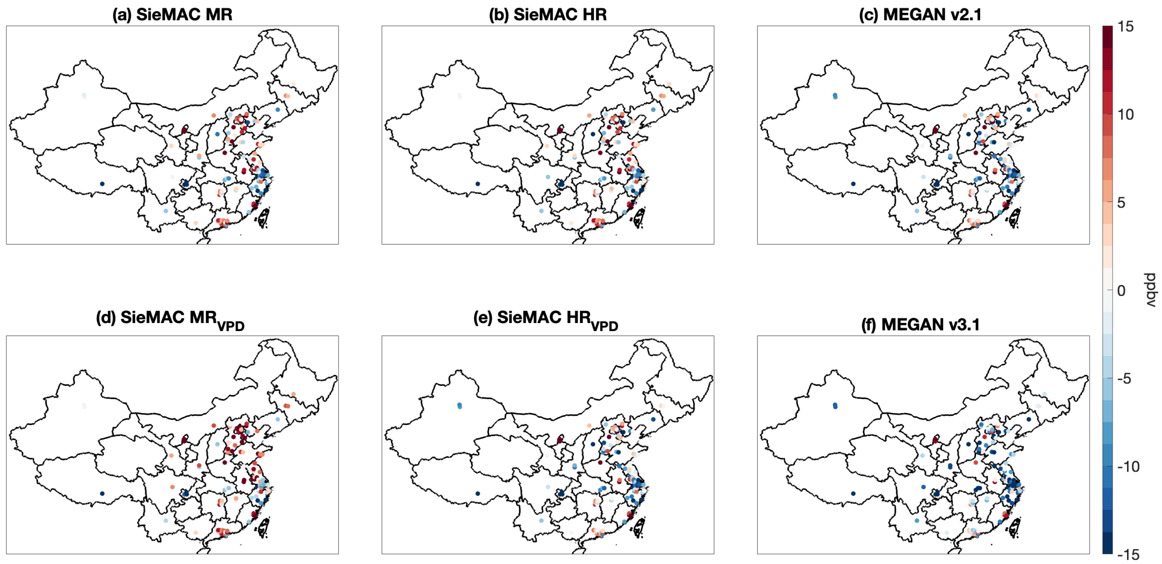

Figure S11. Spatial distribution of MDA8 O_3 mean bias for summer 2013 (all days). Mean bias (model minus observation) at each CNEMC monitoring site for six emission inventories: (a) SieMAC MR, (b) SieMAC HR, (c) MEGAN v2.1, (d) SieMAC MR$_{VPD}$, (e) SieMAC HR$_{VPD}$, and (f) MEGAN v3.1. Colors indicate bias magnitude in ppbv (scale at right); red shades show model overestimation and blue shades show model underestimation relative to observations.

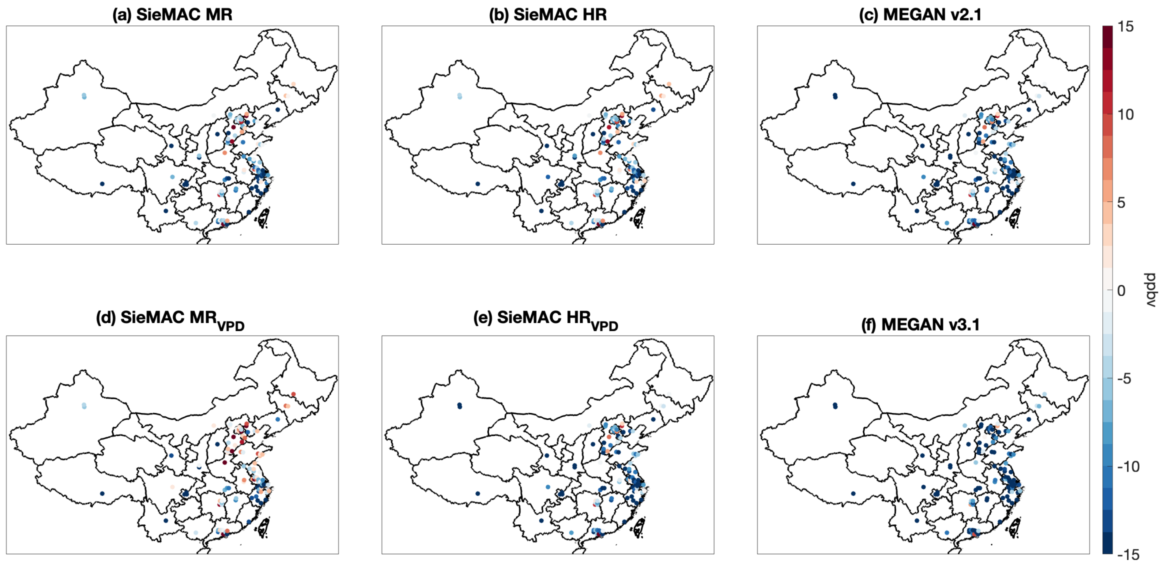

Figure S12. Spatial distribution of MDA8 O_3 mean bias for high ozone days (MDA8 ≥ 60 ppbv). Mean bias (model minus observation) at each CNEMC monitoring site during days when observed MDA8 ozone concentrations exceed 60 ppbv, shown for six emission inventories: (a) SieMAC MR, (b) SieMAC HR, (c) MEGAN v2.1, (d) SieMAC MR$_{VPD}$, (e) SieMAC HR$_{VPD}$, and (f) MEGAN v3.1. Colors indicate bias magnitude in ppbv (scale at right); red shades show model overestimation and blue shades show model underestimation relative to observations.

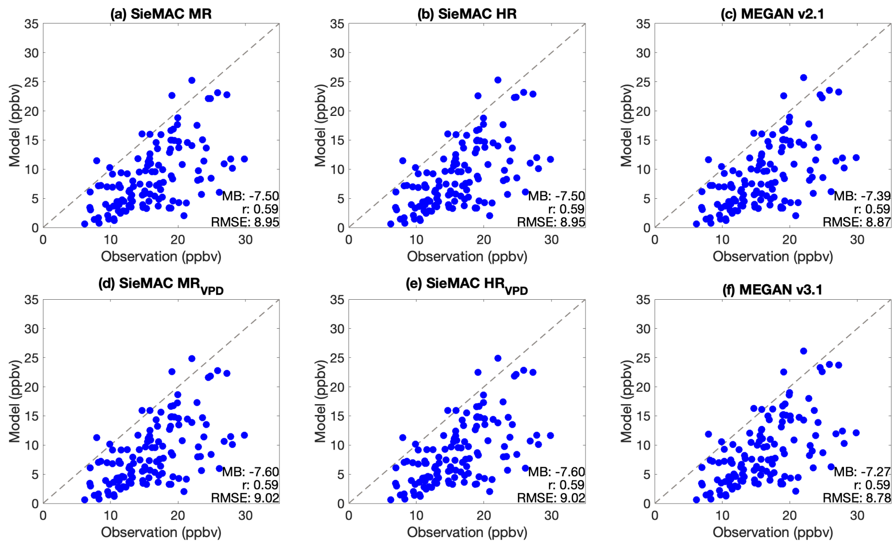

Figure S13. **Evaluation of the REAM simulations for surface nitrogen dioxide (NO_2) during summer 2013**. Scatterplots compare seasonal mean model values with observations from the China National Environmental Monitoring Centre (CNEMC) network at individual sites for six emission configurations: (a) SieMAC MR, (b) SieMAC HR, (c) MEGAN v2.1, (d) SieMAC MR$_{VPD}$, (e) SieMAC HR$_{VPD}$, and (f) MEGAN v3.1. The dashed line denotes the 1:1 relation, and panel annotations give the mean bias (MB), root-mean-square error (RMSE), and Pearson correlation coefficient (r) for each configuration.

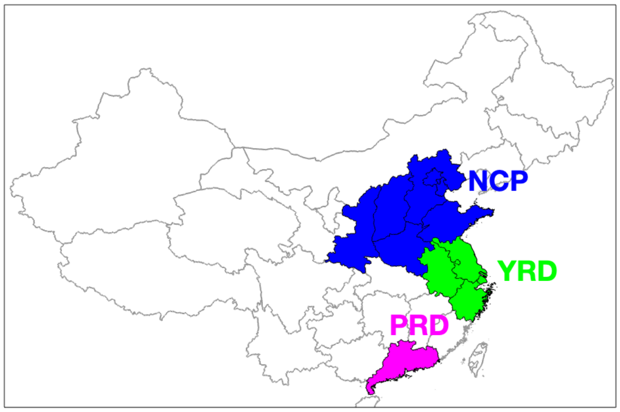

Figure S14. Administrative-map outline showing the three study regions analysed in Section 4.2.2: North China Plain (NCP, blue), Yangtze River Delta (YRD, green), and Pearl River Delta (PRD, magenta)

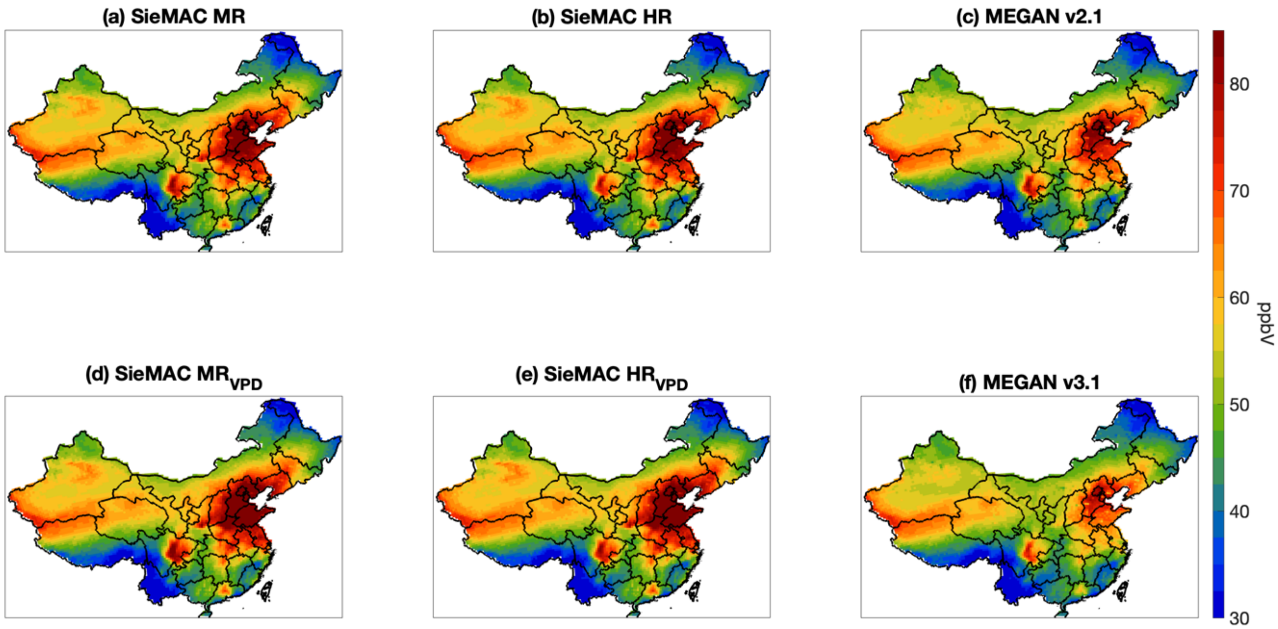

Figure S15. Seasonal mean daily maximum 8-h average ozone (MDA8) for June–August 2013 simulated with six emission inventories: (a) SieMAC MR, (b) SieMAC HR, (c) MEGAN v2.1, (d) SieMAC MR$_{VPD}$, (e) SieMAC HR$_{VPD}$, and (f) MEGAN v3.1. Colours indicate ozone concentration in ppbv (scale at right).

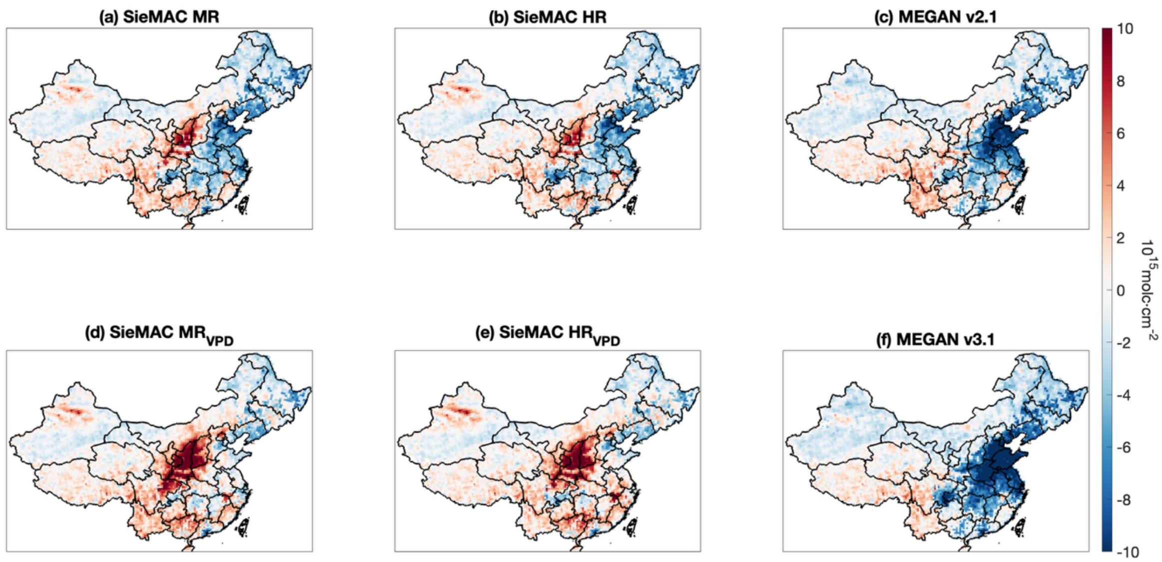

Figure S16. **Spatial bias of summertime (June–August 2013) formaldehyde vertical columns in the model simulations relative to OMI satellite observations**. Panels display model – OMI differences for (a) SieMAC MR, (b) SieMAC HR, (c) MEGAN v2.1, (d) SieMAC MR$_{VPD}$, (e) SieMAC HR$_{VPD}$, and (f) MEGAN v3.1. Colours indicate the bias in 10^{15} molec cm^{-2} (scale at right); warm shades denote model overestimates and cool shades model underestimates.

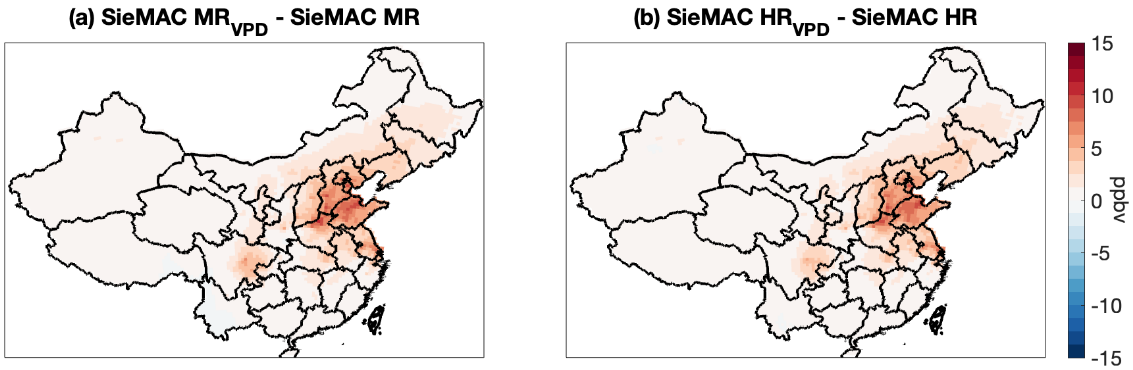

Figure S17. Effect of vapour-pressure-deficit (VPD) stress on summertime (June–August 2013) ozone. (a) shows the change in daily maximum 8-h average ozone (ΔMDA8) obtained by subtracting the unstressed run from the VPD-enabled run at medium resolution (SieMAC MR$_{VPD}$ – SieMAC MR); (b) shows the same difference at high resolution (SieMAC HR$_{VPD}$ – SieMAC HR). Colours denote the VPD-induced ozone change in ppbv (scale at right), with red shades indicating higher concentrations when VPD stress is included and blue shades indicating lower concentrations**.**

References

[1] Klinger, L. F., Li, Q. J., Guenther, A. B., Greenberg, J. P., Baker, B., and Bai, J. H.: Assessment of volatile organic compound emissions from ecosystems of China, Journal of Geophysical Research: Atmospheres, 107, ACH 16-11-ACH 16-21, https://doi.org/10.1029/2001JD001076, 2002.
[2] Wang, X., Situ, S., Chen, W., Zheng, J., Guenther, A., Fan, Q., and Chang, M.: Numerical model to quantify biogenic volatile organic compound emissions: The Pearl River Delta region as a case study, Journal of Environmental Sciences, 46, 72-82, https://doi.org/10.1016/j.jes.2015.08.032, 2016.
[3] Zhao, J., Bai , Y., Wang, Z., and Zhang, S.: Studies on the emission rates of plants VOCs in China, China Environmental Science, 24, 654-647, 10.3321/j.issn:1000-6923.2004.06.004, 2004.
[4] Yang, D., Bai, Y., Li, J., Pan, N., Yu, K., Tang, L., Peng, L., and Xing, S.: Study on hydrocarbon compounds from natural source in the Pearl River Delta area, China Environmental Science, 21, 422-426, 10.3321/j.issn:1000-6923.2001.05.009, 2001.
[5] Geron, C., Owen, S., Guenther, A. B., Greenberg, J., Rasmussen, R., Hui Bai, J., Li, Q.-J., and Baker, B.: Volatile organic compounds from vegetation in southern Yunnan Province, China: Emission rates and some potential regional implications, Atmospheric Environment, 40, 1759-1773, https://doi.org/10.1016/j.atmosenv.2005.11.022, 2006.
[6] Wang, Z., Zhang, S., Lu, S., and Bai, Y.: Screenings of 23 plant species in Beijing for volatile organic compound emissions, Environmental Science, 24, 7-12, 10.3321/j.issn:0250-3301.2003.02.002, 2003.
[7] Song, Y., Zhang, Y., Wang, L., and An, J.: Estimation of biogenic VOCs emissions in Eastern China based on remote sensing data, Acta Scientiae Circumstantiae, 32, 2216-2227, 2012.
[8] Gao, C.: Shade tolerance and photosynthetic characteristics of 15 typical garden ornamental plants in Guangxi region, Jiangsu Agriculture Science, 44, 209-214, 10.15889/j.issn.1002-1302.2016.04.058, 2016.
[9] Wang, Z., Bai, Y., and Zhang, S.: A biogenic volatile organic compounds emission inventory for Beijing, Atmospheric Environment, 37, 3771-3782, https://doi.org/10.1016/S1352-2310(03)00462-X, 2003.
[10] Wang, X., Mu, Y., Ouyang, Z., Zhang, X., Ni, S., and Fu, C.: Study on emissions of isoprene from major plants living in Taihu Basin, Chinese Bulletin of Botany, 19, 224-230, 2002.
[11] Dong, L., Liu, S., Shi, Z., and Feng, Q.: Relationships between leaf traits of Castanopsis species and the environmental factors in the north-south transect of eastern China, Forest Research, 22, 463-469, 10.3321/j.issn:1001-1498.2009.04.001, 2009.
[12] Li, K. and Xiang, W.: Comparison of specific leaf area, SPAD value and seed mass among subtropical tree species in hilly area of Central Hunan, China, Journal of Central South University of Forestry & Technology, 31, 213-218, 10.3969/j.issn.1673-923X.2011.05.037, 2011.
[13] Li, Q. and Klinger, L.: The correlation between the volatile organic compound emissions and the vegetation succssion of the ecosystems in different climate zones of China, Journal of Integrative Plant Biology, 43, 1065-1071, 10.3321/j.issn:1672-9072.2001.10.013, 2002.

[14] Huang, A., Li, N., Guenther, A., Greenberg, J., Baker, B., Graessli, M., and Bai, J.: Investigation on emission properties of biogenic VOCs of landscape plants in Shenzhen, Environmental Science, 32, 3555-3559, CNKI:SUN:HJKZ.0.2011-12-017, 2011.
[15] Wang, Q., Han, Z., Wang, T., and Higano, Y.: An estimate of biogenic emissions of volatile organic compounds during summertime in China, Environmental Science and Pollution Research, 14, 69-75, 2007.
[16] Guenther, A. B., Hewitt, C. N., Erickson, D., Fall, R., Geron, C., Graedel, T., Harley, P., Klinger, L., Lerdau, M., Mckay, W. A., Pierce, T., Scholes, B., Steinbrecher, R., Tallamraju, R., Taylor, J., and Zimmerman, P.: A global model of natural volatile organic compound emissions, Journal of Geophysical Research: Atmospheres, 100, 8873-8892, https://doi.org/10.1029/94JD02950, 1995.
[17] Singh, R., Singh, A. P., Singh, M. P., Kumar, A., and Varshney, C. K.: Emission of isoprene from common Indian plant species and its implications for regional air quality, Environmental Monitoring and Assessment, 144, 43-51, 10.1007/s10661-007-9940-7, 2008.
[18] Situ, S., Wang, X., Guenther, A. B., Zhang, Y., Wang, X., Huang, M., Fan, Q., and Xiong, Z.: Uncertainties of isoprene emissions in the MEGAN model estimated for a coniferous and broad-leaved mixed forest in Southern China, Atmospheric Environment, 98, 105-110, https://doi.org/10.1016/j.atmosenv.2014.08.023, 2014.
[19] Jiang, Q., Long, W., Liu, A., Xiao, X., Liu, Y., Li, C., and Yang, Y.: Changes in leaf structural characteristics of three bamboo species at different altitudes in Mount Emei, Journal of Bamboo Research, 37, 64-72, 10.3969/j.issn.1000-6567.2018.01.011, 2018.
[20] Zhang, L., Bai, Y., Wang, X., Ouyang, Z., Mu, Y., and Miao, Q.: Isoprene emission of bamboo and its implicationn to ozone level in region, Acta Ecologica Sinica, 22, 1333-1338, 10.3321/j.issn:1000-0933.2002.08.024, 2002.
[21] Li, J., Tian, L., Lun, X., Yu, X., and Huang, D.: Emission inventory of botanical volatile organic compounds (BVOCs) in Beijing, Environmental Chemistry, 36, 776-786, 10.7524/j.issn.0254-6108.2017.04.2016072402, 2017.
[22] Lin, H., Chen, S., Guo, Z., Yang, Q., and Gao, P.: Allometric relationship among leaf traits in different stand density of Pleioblastus amarus, Forest Research, 30, 617-623, 10.13275/j.cnki.lykxyj.2017.04.012, 2017.
[23] Li, Y., Yao, J., Yang, S., and Hou, J.: Trait differences research on leaf of liaodong oak forest main species in Dongling mountain, Journal of Beijing Forestry University, 23, 72-77, 2014.
[24] Li, S., Yuan, X., Li, Q., and Feng, Z.: Inventory and characteristics of biogenic volatile organic compounds (BVOCs) for 12 deciduous fruit trees, Environmental Science, 40, 2078-2085, CNKI:SUN:HJKZ.0.2019-05-010, 2019d.
[25] Jin, M., Jiang, F., Jin, G., and Liu, Z.: Variations of specific leaf area in different growth periods and canopy positions of Betula platyphylla at different ages, Scientia Silvae Sinicae, 54, 18-26, 10.11707/j.1001-7488.20180903, 2018.
[26] Lian, Z., Zhang, C., Cheng, Y., and Xin, B.: Geographical variations of functional traits of typical tree species in northeastern China, Journal of Beijing Forestry University, 41, 42-48, 10.13332/j.1000-1522.20180352, 2019.
[27] Bao, H.: Presumpition of biogenic volatile organic compounds emissions from greening tree species and its emission rate classification in Hohhot, Inner Mongolia Petrochemical Industry, 11, 1-4, CNKI:SUN:NMSH.0.2015-11-001, 2015.
[28] Zhang, G. and Xie, S.: Estimation of VOC Emission from Forests in China Based on the Volume of Tree Species, Environmenal Science, 30, 2816-2822, 10.3321/j.issn:0250-3301.2009.10.002, 2009.
[29] Wang, H., Wu, Q., Liu, H., Wang, Y., Cheng, H., Wang, R., Wang, L., Xiao, H., and Yang, X.: Sensitivity of biogenic volatile organic compound emissions to leaf area index and land cover in Beijing, Atmos. Chem. Phys., 18, 9583-9596, 10.5194/acp-18-9583-2018, 2018.
[30] Li, J., He, J., Sun, Y., Zhao, A., and Tian, Q.: Physiological and ecological responses of ten garden plant functional traits to air pollution, Ecology and Environmental Sciences, 29, 1205-1214, 10.16258/j.cnki.1674-5906.2020.06.017, 2020.
[31] Luo, T., Luo, J., and Pan, Y.: Leaf traits and associated ecosystem characteristics across subtropical and timberline forests in the Gongga Mountains, Eastern Tibetan Plateau, Oecologia 142, 261-273, https://doi.org/10.1007/s00442-004-1729-6, 2005.
[32] Zhu, Y.: Study on plant-based VOC emissions in subtropical urban and rural areas, Zhejiang University, 2011.
[33] Pan, Y., Chen, X., Jiang, Y., Liang, S., Lu, Z., Huang, Y., Ni, M., Qin, C., and Liu, R.: Changes in leaf function traits and soil environmental factors in response to slope gradient in Karst hills of Guilin, Acta Ecologica Sinica, 38, 1581-1589, 10.5846/stxb201701210173, 2018.
[34] Tsui, J. K.-Y., Guenther, A. B., Yip, W.-K., and Chen, F.: A biogenic volatile organic compound emission inventory for Hong Kong, Atmospheric Environment, 43, 6442-6448, https://doi.org/10.1016/j.atmosenv.2008.01.027, 2009.
[35] Pang, S., Ou, Z., Shen, W., He, F., and Lu, G.: Leaf functional traits variations and adaptive strategies of dominant woody economic plants in karst area of Southwest Guangxi, Guihaia, 41, 707-714, 10.11931/guihaia.gxzw202002005, 2021.
[36] Deng, L., Wang, H., Shangguan, Z., and Liu, G.: Variations of specific leaf area and nutrients of Chinese caragana in the Loess Plateau region suffering both wind and water erosions, Acta Ecologica Sinica, 30, 4889-4897, 2010.
[37] Li, J., Xu, C., Zhu, J., Wang, X., Chen, Z., and Zhao, K.: Phenotypic adaptation strategy of Cotinus coggygria seedings in continuous drought environments, Journal of Northwest Forestry University, 34, 28-34, 10.3969/j.issn.1001-7461.2019.02.05, 2019.
[38] Chen, X., Zhang, Z., Yang, L., Yun, Y., Chen, J., and Zheng, D.: Effects of light intensity on phenotypic plasticity and survival strategy of Dracaena cambodiana seedlings, Journal of Tropical and Subtropical Botany, 26, 150-156, 10.11926/jtsb.3782 2018.
[39] Liu, T., Liu, G., Zhang, M., Luo, H., He, Z., Gao, T., and Chen, F.: Analysis of structural traits and nitrogen-phosphorus nutrient content in leaves of wild Elaeagnus glabra, Chinese Wild Plant Resources, 3, 20-24, 10.3969/j.issn.1006-9690.2020.03.004, 2020.

[40] Chen, Y., Li, D., Shi, Y., and He, X.: Emission rate of biogenic volatile organic compounds from urban trees in Shenyang, China, Journal of Northeast Forestry University, 37, 47-49, 2009.
[41] Kang, B., Liu, J., Xu, X., and Bu, X.: The specific leaf weight of some common tree species in Loess Plateau area and its relationship with photosynthetic capacity, Journal of Southwest Forestry University, 25, 1-4,11, 10.11929/j.issn.2095-1914.2005.02.001, 2005.
[42] Wang, T., Guo, J., Liu, N., and Zhang, Y.: Photosynthetic and Morphological Responses and Plasticity of Four Naturally-Regenerated Shrubs under Forest Light Environments, Scientia Silvae Sinicae, 47, 56-63, 2011.
[43] Tang, Q., Huang, Y., Ding, Y., and Zang, R.: Interspecific and intraspecific variation in functional traits of subtropical evergreen and deciduous broad-leaved mixed forests, Biodiversity Science, 24, 262-270, 10.17520/biods.2015200, 2016.
[44] Peng, C., Song, M., Zhou, C., Li, Y., Li, X., and Cao, G.: Relationship between Leaf Functional Traits of Herbaceous Plants and Soil Factors in Different Coverage Gradients of Potentilla fruticosa Shrub under Grazing, Acta Botanica Boreali-Occidentalia Sinica, 40, 870-881, 10.7606/j.issn.1000-4025.2020.05.0870, 2020.
[45] Yang, L., Shao, D., and Luan, Z.: Variation in leaf functional traits of Rhododendron aureum with altitude in the Changbai Mountains, Jiangsu Agriculture Science, 41, 3, CNKI:SUN:JSNY.0.2013-09-060, 2013.
[46] Bu, Q., Hou, Y., Fang, H., Zhang, Z., and Bai, X.: Eco-Physiological characteristics of the exotic plant Rhus typhina in comparison with its indigenous congeners Rhus chinensis, Scientia Silvae Sinicae, 53, 1-7, 10.11707/j.1001-7488.20170501, 2017.
[47] Yin, L., Li, S., Zhou, M., Wang, Q., Wu, Y., and Luo, P.: Effect of Grazing Interference on the Architecture of Sibiraea angustata in the Eastern Qinghai Tibetan Plateau, Bulletin of Botanical Research, 30, 737-741, 10.7525/j.issn.1673-5102.2010.06.020, 2010.
[48] Wang, H., Liu, N., Yao, Y., Xie, W., and Wang, L.: The Relationship between Foliar TOC of Tamarix chinensis Lour. and nutrient elements' content in saline-alkali soil of North Shanxi, Ecology and Environmental Sciences, 26, 2036-2044, 10.16258/j.cnki.1674-5906.2017.12.006, 2017.
[49] RodrÍGuez, L. G. and PÉRez, M. R.: Recent changes in Chinese forestry seen through the lens of Forest Transition theory, The International Forestry Review, 15, 456-470, 2013.
[50] Zhang, X.: Vegetation map of the People's Republic of China (1:1 000 000), Geology Press, Beijing2007.